

## Deformation of 921 Earthquake by Satellite Radar Interferometry: Co-seismic and Post-seismic Estimation

L. S. Liang<sup>1</sup>, C. T. Wang<sup>1</sup>, K. S. Chen<sup>1</sup>, Y. B., Tsai<sup>2</sup>, A. J. Chen<sup>1</sup>

<sup>1</sup>Center for Space and Remote Sensing Research  
National Central University, Chung-Li, Taiwan

<sup>2</sup>College of Earth Science,  
National Central University, Chung-Li, Taiwan

Tel: 886 – 3 – 4227151 ext. 7625; Fax: 886 – 3 – 4255535

E-mail: lsliang@csrsr.ncu.edu.tw

**KEY WORDS: SAR, INRRERFEROMETRY, EARTHQUAKE**

### ABSTRACT

A major earthquake ( $M_L=7.3$ ) has occurred near the small town Chi-Chi in the Nantou County, Taiwan, at 1:47 a.m. local time on September 21, 1999 (17:47 GMT on 20 September). The epicenter was 12.5 km northwest the Sun-Moon lake. The focal depth is 8 km. The death toll has exceeded 2100 and is mounting during the first week after the main shock. In this study, we mainly focus on the there are numerous aftershocks; some of which reach magnitudes of  $M_L = 6.8$ . In this paper we used 8 scenes (1998/01/01, 1999/01/21, 1999/05/06, 1999/06/10, 1999/07/15, 1999/09/23, 1999/10/28, 2000/01/06) of ERS2 images and an external DTM data, by the means of two passes SAR differential interferometry, to detect the deformations before and after the Chi-Chi earthquake. The results based on the available image sets show that prior to the earthquake, it has no clear deformation signature in the interferogram and there are slight displacements in the east of Chelungpu fault; and the displacement areas of the two pairs of DINSAR (1999/10/28 – 1999/09/23; 2000/01/06 – 1999/10/28) were at the same place. The former had about 5.6 cm deformation in slant range, while the latter was about 3 cm. These post-seismic deformations may be due to gravity effects, or the theory of elastic rebound.

### INTRODUCTION

Earthquake produces field displacement near the fault that slipped during a seismic rupture [Bolt,1988]. Measurement of the displacement is important because it provides insight into the geometry of the rupture fault and energy released by the earthquake. According to a report of Central Weather Bureau (CWB), a major earthquake ( $M_L=7.3$ ) has occurred near the small town Chi-Chi in the Nantou County, Taiwan, at 1:47' a.m. local time on September 21, 1999 (17:47 GMT on 20 September). The epicenter was 12.5 km northwest the Sun-Moon lake. The focal depth is 8 km. The death toll has exceeded 2100 and is mounting during the first week after the main shock. The Chi-Chi earthquake essentially was resulted from a major reverse fault, the Chelungpu Fault, trending N-S to NNE-SSW, one of the major trust faults in the deformation front of the fold-and-thrust belt of the Taiwan orogenic belt. The movement of the earthquake produced a linear zone of surface ruptures, extending about 80 km long from north to south. According to the in-situ field investigations, the surface break shows large vertical as well as horizontal displacements, ranged from 1 to 8 meters, along the fault line as a consequence of the Chi-Chi earthquake.

SAR not only obtains the radar scattering coefficient of the land cover, but also carries the phase information about the target when a pair of data is coherently processed. The phase has two major parts: the characteristics of

the land cover itself and the distance between radar and the surface height. A single-phase echo essentially bears no information. Therefore, one must have at least one image pair with the same measuring direction and near the same measuring position to examine the difference of echoes. If the characteristics of the land cover change little during the period of images taken, we can ignore the influence of phase caused by it, and then get the radar interferogram produced by the difference of the measuring distance. We then calculate the difference of the distance by using the interferometric image pairs, and furthermore we use the differential interferograms with the same area but at different time to calculate the height changes and the crustal movements. The use of interferometric synthetic aperture radar (InSAR) for monitoring earth deformation process has received considerable attention. Several studies suggest the great potential of InSAR technique for mapping co-seismic movement associated strong earthquake [Massonnet et al, 1993; Zebker, et al., 1994; Murakami et al, 1996; Wang et al., 2000]. With the microwave frequency, the surface changes can be detected within a centimeter scale. A number of studies have been reported to demonstrate the potential and capability of satellite radar interferometry for surface deformation mappings. For small-scale surface height movements, the differential radar interferometry is usually adopted. For example, Liang et al.[2001] used differential radar interferometry to measure the land subsidence over the west coast of Taiwan and were able to cross-check with the GPS measurements. Similar examples can be found in the references list and reference cited therein. One of the features that make radar interferometry so attractive is inference of surface deformations at high resolution on the ground in global and synoptic scale, which means the mapping can be done shortly after satellite image data takes under favorable conditions. Demonstrated applications of such technique include generation and updating of digital elevation maps, deformation measurement, earthquake monitoring, and plate tectonics.

There are ERS1/2 SAR images acquired and processed. We select a total of 8 scenes (1998/01/01, 1999/01/21, 1999/05/06, 1999/06/10, 1999/07/15, 1999/09/23, 1999/10/28, 2000/01/06) of ERS2 images before and after the 921 Earthquake for extracting the surface displacement. Prior to the 921 earthquake, there are also some great earthquakes that may present some indications on the surface. To identify the precursory signatures associated with the land deformation in gradual trend and to map the possible deformations aftershocks, we have 5 scenes of SAR images to form 3 pairs of differential SAR interferogram ( 1999/05/06 – 1999/01/21, 1999/07/15 – 1999/06/10, 1999/07/15 – 1998/01/01 ), and after the earthquake, we select 3 scenes to form 3 pairs (1999/10/28 – 1999/09/23, 2000/01/06 – 1999/09/23, 2000/01/06 – 1999/10/28 ). The total image pairs we used are listed in the Table 1. The table also shows the perpendicular and parallel baseline values and the corresponding time lag of the pair images.

Table 1: Characteristics of the DIFSAR ERS-2, 3123/232 pairs

	Master	Slave	lag(day)	$B_{//}$ (m)	$B_{+}$ (m)
Pair-1	1999/05/06	1999/01/21	105	-91	-96
Pair-2	1999/07/15	1999/06/10	35	-30	-156
Pair-3	1999/07/15	1998/01/01	560	-29	86
Pair-4	1999/09/23	1999/01/21	245	-145	-309
Pair-5	1999/10/28	1999/05/06	175	37	6
Pair-6	1999/10/28	1998/01/01	665	-80	-156
Pair-7	1999/10/28	1999/09/23	35	91	219
Pair-8	2000/01/06	1999/10/28	70	49	106
Pair-9	2000/01/06	1999/09/23	105	140	325

## TEST SITE, DATA AND PROCESSING

The test site is located at the central area of Taiwan, which belongs to track 232 and frame 3123 of ERS2. SAR studies over this area were also carried out by Wang et al.[2000], Deffontaines et al.[2000], Takeuchi et al.[2000]. Figure 1 shows the interferogram of the test site acquired on May 6 and Jan. 21, 1999. The color coding is: The red band is the amplitude of the master mage, the green band is the phase image, and the blue band is the coherence. It is geocoded, overlapped by the vectors of fault ( cyan color line ) and boundary of country and towns( violet color line ). At the center of the image is location of Taichung city, and the epicenter is indicated by a “ \* “, located in the lower-right part of the image.

A total of 8 pairs of SAR data were processed from single-look complex (SLC) images, to generate co-registered images, coherence images, and differential interferograms using two pass radar Interferometry technique. The external digital elevation model (DEM) with 40 m by 40 m in X-Y posting is made available for this purpose.

## EXTRACTION OF LAND DISPLACEMENT

The pair-1, pair-2, and pair-3 in Table 1 were acquired before the earthquake, and the corresponding differential interferogram images are shown in Figure 1, 2, 3, respectively, where the longest time lag is 560 days. These images were overlaid onto the GIS data layers including the fault vectors. From the interferogram fringes, it seems that there are no clear deformations presented over the central area of Taiwan. A series of quakes prior to the Chi-Chi Earthquake from 1 January, 1999 with their epicenters are displayed in Fig. 4. These quakes seem not triggering large scale deformations detectable in interferograms. It is too early to state at this point that any precursory signal associated with the Chi-Chi Earthquake, if any, is detectable by InSAR technique. More data sets and ground truth are required to evident it.

Pair-4, pair-5, and pair-6 in Table 1 cover the period of pre- and post-seismic with longest time lag of 665 days. In Figures 5, 6, 7, we show the differential interferogram images for these pairs. The phase patterns in these interferograms indicate the phase differences due to land displacement in the slant range direction after removal of the orbital and topography effects. Note that one cycle of fringe is 2.8 cm for C-band SAR.

From these interferograms of Figures 5, 6, and 7, a series of about 11 complete fringes to the west of the Chelungpu fault were able to identify; these fringes are apparently correlated with the displacements triggered by the Chi-Chi Earthquake. Table 2 includes the GPS data of the subsidence part from the reports of Central Geological Survey ( CGS ). After projecting the GPS measurements onto slant range, the comparison of displacement between the GPS and DSAR are reasonable well.

Table 2: The vertical component of displacement of GPS and DSAR.

Site	Longitude	Latitude	GPS dh (cm)	Slant range dh (cm)
AF01	120.5547	23.7706	-11.3	-10.4
AF04	120.5264	23.8732	-14.7	-13.5
AF09	120.506	24.0391	-12.8	-11.8
AF11	120.6763	23.8962	-23.3	-21.4
AF13	120.6895	23.9483	-29.0	-26.7
AF14	120.635	24.0168	-15.4	-14.2
AF15	120.640	24.0960	-18.4	-16.9
AF16	120.660	24.0382	-15.1	-13.9
AF17	120.624	24.1583	-13.7	-12.6

AF18	120.519	24.2178	-5.1	-4.7
AF21	120.564	24.2182	-3.9	-3.6
AF26	120.643	24.2235	-10.1	-9.3
AF28	120.5925	24.0178	-8.6	-7.9
CPUL	120.6266	23.9293	-18.3	-16.8
G041	120.6783	23.7478	-23.1	-21.3
G090	120.554	24.3131	4.7	4.3
G097	120.8641	24.4293	-3.5	-3.2
G098	120.9009	24.2928	-24.3	-22.4
HTZS	120.9739	23.9757	-62.8	-57.8
WNTS	120.5763	24.1399	-10.0	-9.2

The pair-7, pair-8, and pair-9 in Table 1 cover the mapping after the earthquake; Pair-7 has the shortest time lag as well as the shortest perpendicular base line. It is shown that the differential interferogram image is distinctly as given in Figure 8, 9, and 10. Figure 8 is the differential interferogram of Oct. 28 and Sep. 23, 1999. We can find in Figure 8 that there are about 3 fringes in Sin-She county and two fringes in Cao-Tun city. Similar fringes are also illustrated at the same area, as displayed in Figure 9, except there is only one fringe. As time goes on, it seems less likely to identify the fringes in the same area, as given in Fig.10. The fringes are not well structured and organized, indicating less and less deformations occur. The phenomena may be explained by gravity effects, or the theory of elastic rebound.

### Conclusions

- (1) For pre-seismic, from three pairs( pair-1, pair-2, pair-3 ) of differential SAR interferograms, it has no clear displacement signature derived from interferograms over the interested areas. Further investigations seems needed to clarify this. One possibility is that there are many kinds of well grown vegetation in west of Chelunpu, and the east part is steep mountains with forest and some luxuriant fruit trees, which make C-band SAR more difficult to detect the possible deformations.
- (2) For inter-seismic period, from pair-4, pair-5, pair-6 interferograms, there are clear deformations pattern recognized from the interferograms, even for time lag as long as 665 days, and the perpendicular base line being 309 meters. There are no fringes over the east of Chelunpu fault. Possible causes are the deformation scale is too large to be detected in SAR which is sensitive to small changes in wavelength (cm) scale.
- (3) For post-seismic, aftershock surface deformations are detectable.

### REFERENCES

1. Bolt, B. A., *Earthquakes*, W. H. Freeman and Company, New York, NY, 1988.
2. Wang,C.T., L.S. Liang, K. S. Chen, A.J.Chen, 2000, "A Study of Surface Deformation From Earthquake by Differential Radar Interferometry", *Proceedings of the 21<sup>st</sup> Asian Conference on Remote Sensing*, pp. 866-871.Dec. 4-8, 2000, Taipei, Taiwan.
3. Deffontaines B., Liang L.S., Pathier E., Wang C.T., Fruneau B., Lee C.T., Raymond D. J. Angelier and Rudant J.P., 2000, " 921 CHICHI Earthquake: Preliminary Interferometric Interpretation ", *Proceedings of the 21<sup>st</sup> Asian Conference on Remote Sensing*, pp. 755-760, Dec. 4-8, 2000, Taipei, Taiwan.
4. Liang L.S., Wang C.T., Chen K.S., Hou C.S., 2001, " A Study On Differential Interferometry in Subsidence", *Proceedings of the fourth groundwater resource and water quality protection*, pp. 191-195, Apr. 13, 2001.

5. Massonnet, D. and T. Rabaute, "Radar interferometry: limit and potential;" *IEEE Trans. Geoscience and Remote Sensing*, vol.31, no.2, pp.455-464, 1993.
6. Murakami, M., M. Tobita, S. Fujiwara, T. Saito, and H. Masahru, "Coseismic crustal deformations of the 1994 Northridge, California, earthquake detected by interferometric JERS-1 synthetic aperture radar," *J. Geophys. Res.*, vol. 101, pp. 8605-8614, 1996
7. Takeuchi, Shoji, Yuzo Suga, and Yoshinari Oguro 2000, "Verification of InSAR Capability For Disaster Monitoring – A Case Study on Chi-Chi Earthquake in Taiwan", *Proceedings of the 21<sup>st</sup> Asian Conference on Remote Sensing*, pp. 738-743, Dec. 4-8, 2000, Taipei, Taiwan.
8. Zebker, H. A., P. A. Rosen, R. M. Goldstein, A. Ggriell, and C. L. Werner, "On the derivation of coseismic displacement field using differential radar interferometry: The Landers earthquake," *J. Geophys. Res.*, vol. 99, pp.19617-19634, 1994

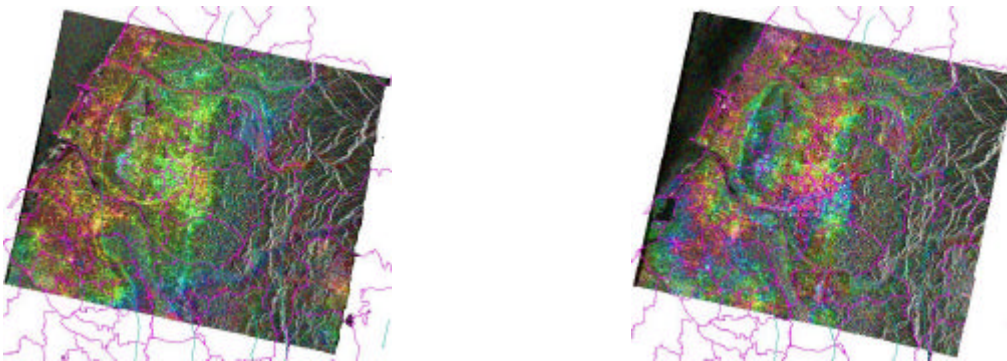


Fig. 1 (Left): The geo-coded differential interferogram image of May 6 and Jan. 21, 1999.

Fig. 2( Right ): Interferogram image of Jul. 15 and Jun. 10, 1999.

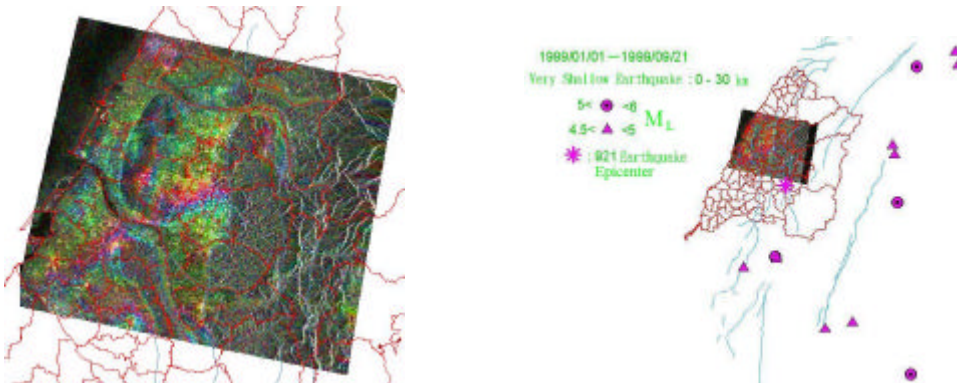


Fig. 3 ( Left): Interferogram image of Jul. 15 and Jan. 1, 1998. Fig. 4 ( Right ): The epicenters for magnitude great than 4.5 of the very shallow earthquake( 0 – 30 km ) between Jan. 01 and Sep. 21, 1999( local time )

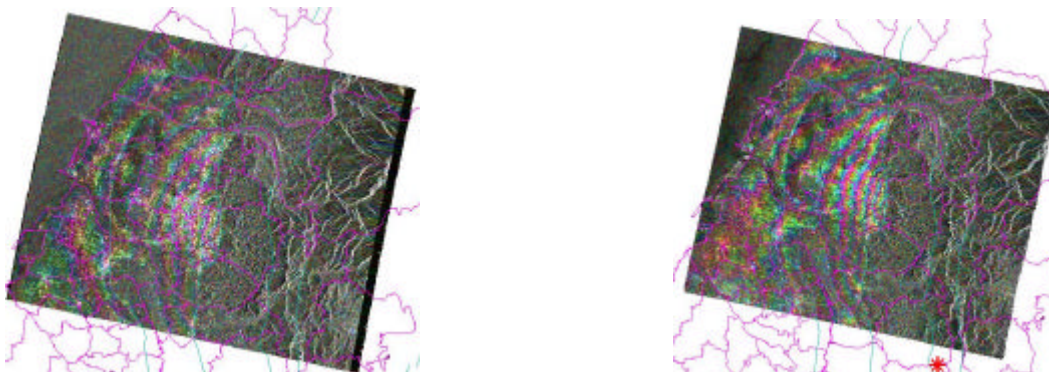


Fig. 5 ( Left ) The differential interferogram image of Sep. 23, and Jan. 21, 1999.

Fig. 6 (Right): The differential interferogram image of Oct. 28, and May 6, 1999.

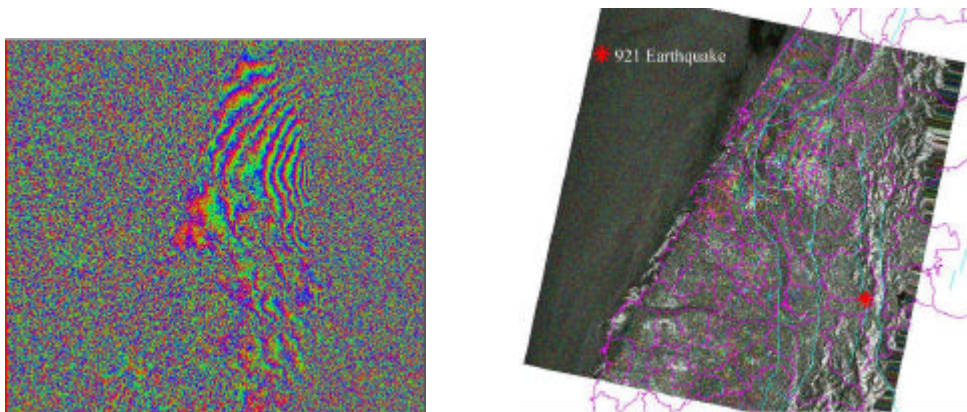


Fig. 7 (Left): The differential interferogram image of Oct. 28, 1999 and Jan. 1, 1998; right figure is geocoded.

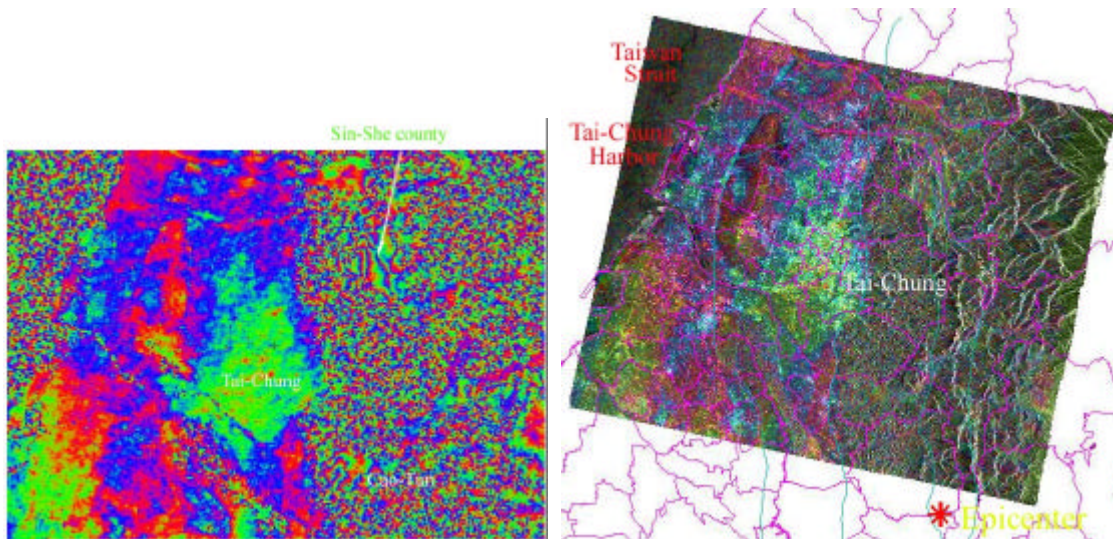


Fig. 8 (Left ) : The differential interferogram image of Oct. 28 and Sep. 23, 1999, right figure is geocoded image.

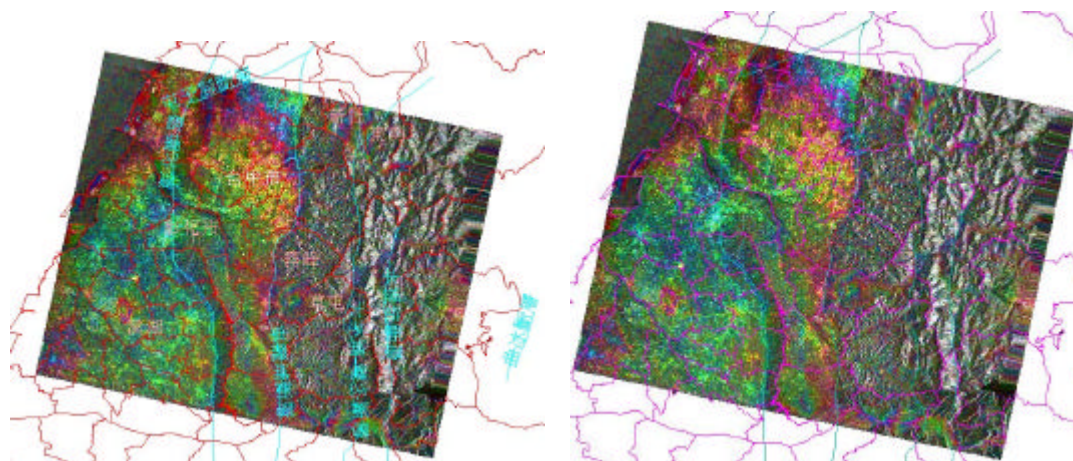


Fig. 9 (left): The differential interferogram image of Jan. 6, 2000 and Oct. 28, 1999.

Fig. 10(Right): The differential interferogram image of Jan. 6, 2000 and Sep. 23, 1999.